Shahrood University of Technology

Journal of Mining and Environment (JME)

Journal homepage: www.jme.shahroodut.ac.ir

Iranian Society of Mining Engineering (IRSME)

Challenging Microbubble Assumptions: Modeling and Optimizing Coarse Quartz Flotation in a Cationic Environment

Ahmed Abbaker[1,3*], and Nevzat Aslan[2]

1. Mining Engineering Department, Graduate School of Natural and Applied Sciences, Sivas Cumhuriyet University, 58140 Sivas, Türkiye
2. Industrial Engineering Department, Sivas Cumhuriyet University, 58140 Sivas, Türkiye
3. Department of Mining Engineering, Faculty of Engineering Sciences, Omdurman Islamic University, P.O.BOX Khartoum 10257, Omdurman 382, Sudan

Article Info

Received 9 August 2024
Received in Revised form 21 September 2024
Accepted 18 November 2024
Published online 18 November 2024

DOI: 10.22044/jme.2024.14917.2839

Keywords

Coarse particle flotation
Microbubble-assisted flotation
Cationic environment
Optimization
Modeling

Abstract

This work optimizes coarse particle flotation using microbubble-assisted flotation in a cationic environment created by dodecylamine (DDA). The flotation efficiency of coarse quartz particles (D50 = 495 µm) was investigated through an examination of the interactions between microbubbles (20-30 µm), the cationic environment, and various operational parameters. A systematic approach utilizing factorial and Box-Behnken experimental designs was employed to evaluate the effects of the multiple variables. These variables included the dodecylamine (DDA) concentration, methyl isobutyl carbinol (MIBC) concentration, impeller speed, pulp density, the addition of fine particles, and the presence of microbubbles. The DDA concentration and the impeller speed significantly impacted the coarse particle recovery, while microbubbles increased recovery by 15% under non-optimized conditions; optimization revealed a more negligible difference. The optimized conditions achieved maximum recoveries of 99.47% and 97.88% with and without microbubbles, respectively, indicating the minimal effect when other parameters were optimized. This research work shows that a careful optimization of the flotation parameters can achieve high coarse particle recovery rates, with microbubbles playing a less significant role than anticipated. These findings suggest that optimizing the conventional parameters may be more crucial than the microbubble introduction for enhancing the flotation efficiency of larger particles. The work contributes to our understanding of coarse particle flotation, and provides insights for improving the mineral processing techniques for challenging the particle sizes.

1. Introduction

Mineral processing is integral to the global resource industry, with froth flotation being a key and versatile separation technique. However, froth flotation efficiency is significantly reduced when processing coarse particles, presenting a major challenge in mineral beneficiation. Conventional flotation is most effective within a particle size range of 10 to 150 µm, depending on the particle density [1]. This limitation often necessitates energy-intensive and costly pulverization processes, substantially increasing the overall expenses in mineral processing operations [2]. Several factors impede the flotation of coarse particles, primarily the low attachment efficiency and high detachment potential, leading to poor recovery rates [3, 4]. Additionally, the high density of coarse particles causes them to settle at the bottom of flotation cells, further complicating the recovery [5, 6]. Although high-turbulence environments in mechanical cells are necessary for particle suspension, they paradoxically destabilize the bubble-particle aggregates [7]. These challenges reduce the recovery rates, and have broader implications for energy consumption and environmental sustainability in the mining industry. Expanding the effective particle size range in the flotation processes offers multi-faceted benefits throughout the mineral processing operations. Enabling the flotation of coarser particles (e.g. 300 µm versus the conventional 100 µm) could potentially reduce the comminution energy

Corresponding author: a7medelmubarak@oiu.edu.sd (A. Abbaker)

consumption by 30-50%. This significant reduction in the grinding requirements not only conserves energy but also minimizes the generation of fine particles. Consequently, downstream processes such as drying, thickening, and filtration become more efficient, and economically viable. Depending on the specific ore characteristics, the advanced flotation techniques could potentially allow for an increase in the maximum particle size to around 500 μm. This approach might enable the separation of a substantial portion of the feed material through an initial coarse flotation stage. Subsequently, the coarse concentrate could be reground to a finer size that aligns with the ore's inherent liberation properties, ensuring optimal mineral recovery in the final product [5].

A recent research work has explored various approaches to improve coarse particle flotation, though significant challenges remain. Hassanzadeh et al. and Nazari et al. (2022) investigated novel flotation cell designs. However, they noted limited industry adoption due to high implementation costs and associated risks, underscoring the difficulty of translating laboratory innovations into industrial practice [8, 9]. Farrokhpay et al. (2011) reviewed the strategies such as the Eriez HydroFloat and Woodgrove SFR, emphasizing the need for more research work on the hydrodynamics of these systems in industrial settings [10]. Efforts to optimize fluidized-bed flotation cells have encountered persistent issues like low recovery rates and frequent particle detachment. While Kromah et al. (2022) reported an improved recoveries for particles up to 850 μm using the HydroFloat technology, they also highlighted challenges in maintaining stable froth layers with coarse particles, reflecting the complexity of the froth stability mechanisms in such systems [11]. Jameson (2010) emphasized the need for a deeper understanding of enhanced hydrophobicity mechanisms in coarse particles, particularly at the molecular level of collector-mineral interactions [5].

A comprehensive review by Anzoom et al. (2024) provides valuable insights into the current state of coarse particle flotation [12]. Their study summarized the recent advances, ongoing challenges, and potential solutions in this field. They highlighted the promising technologies such as hybrid flotation cells, fluidized bed separators, and bubble-particle aggregate flotation. The review also emphasized the need for further research works in areas like the bubble-particle interaction mechanisms, froth stability with coarse particles, and the development of more efficient collectors and frothers tailored for coarse particle flotation. This work underscores the complexity of coarse particle flotation, and the multi-faceted approach required to advance this technology in the industrial applications.

One promising avenue is the use of microbubbles in the flotation processes. Microbubbles, with their larger surface area and lower rising velocity than the conventional bubbles, have shown the potential to enhance particle attachment, and reduce the collector consumption [13, 14]. These small bubbles do not directly lift coarse particles. Instead, they act as a 'bridge' or 'secondary collector', adhering to particle surfaces, and increasing their hydrophobicity (Figure 1). This mechanism promotes more effective attachment to larger conventional bubbles, potentially improving the overall flotation performance. Fan et al. (2012) demonstrated the improved fine particle recovery using microbubbles but also revealed the complexity of microbubble stability in the presence of coarse particles and high-shear environments typical of industrial flotation cells [15]. Nazari et al. (2018) explored the impact of nanobubbles (NBs) on the coarse quartz particle flotation, observing a significant enhancement in the recovery rates. Their study found that NBs increased the recovery of particles in the size range of -425 + 106 μm by an average of 14%, with an optimal performance at lower Reynolds numbers, and in conjunction with larger conventional bubbles [16]. A further research work by Nazari et al. (2019) under various hydrodynamic conditions revealed even more promising results, with NBs facilitating up to a 21% improvement in the flotation recovery, and a 36% increase in the flotation rate constants, achieving maximum recoveries of 97.5-98% across different impeller configurations [14].

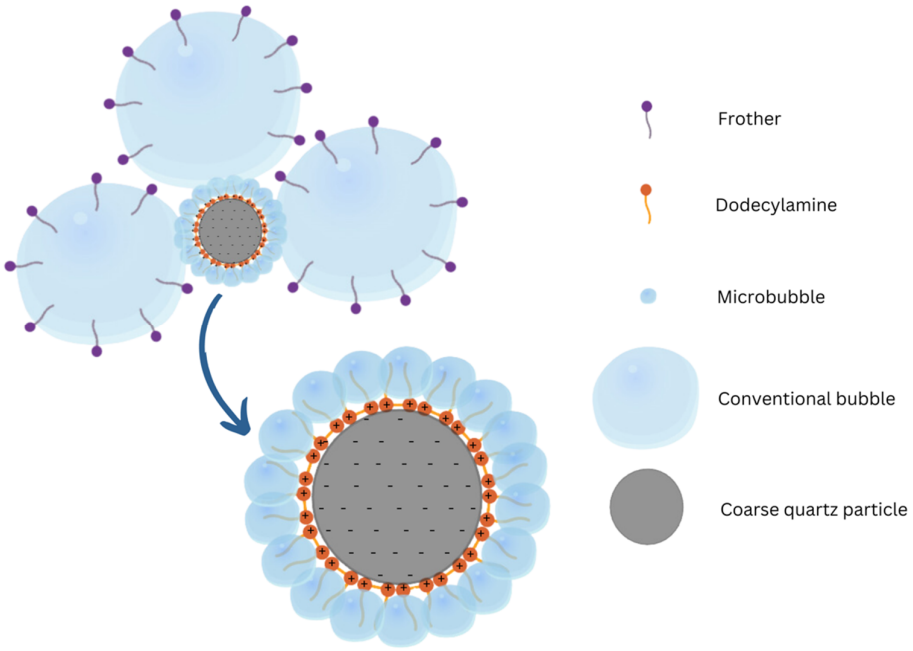

Figure 1. Schematic representation of nano/microbubble-assisted flotation mechanism.

Recent advancements in the nanobubble technology have further expanded our understanding of their potential in froth flotation. Tao (2022) conducted a comprehensive review of the recent advances in nanobubble-enhanced froth flotation [17]. This study highlighted the significant improvements in the flotation performance across various minerals and particle sizes when using nanobubbles. The key findings included an enhanced particle-bubble attachment efficiency and a reduced collector consumption. The review also discussed the mechanisms behind nanobubble-enhanced flotation, including increased hydrophobicity of mineral surfaces and improved froth stability. These insights suggest that the nanobubble technology could be particularly beneficial for coarse particle flotation, where the conventional methods often struggle.

Building on this work, Zhou et al. (2022) investigated the combined effects of micro- and nano-bubbles on quartz flotation [18]. Their study revealed a synergistic effect when using both bubble sizes together. The combination of micro- and nano-bubbles led to an improved flotation recovery and kinetics, particularly for fine particles. This research work suggests that a multi-scale bubble approach could potentially address some of the challenges in coarse particle flotation by enhancing the overall flotation efficiency across a broader range of particle sizes.

Despite these advances, the exact mechanisms by which NBs enhance coarse particle flotation remain unclear, necessitating a further investigation into the fundamental interactions between NBs, conventional bubbles, and coarse particles. Filippov et al. (2010) highlighted the complex interplay between particle size, bubble size, and surface forces in fine and coarse particle flotation, noting the limitations of the current models in accurately predicting the microbubble behaviour in coarse particle flotation systems, particularly concerning the attachment efficiency and froth stability [19]. In addition to the microbubble technology, the choice of collector is crucial for optimizing froth flotation, especially for coarse particles [20]. Cationic collectors such as dodecylamine (DDA), demonstrate a high selectivity in specific mineral systems, allowing for more efficient separation of valuable minerals from gangue. DDA provides several advantages including strong adsorption onto mineral surfaces, high selectivity in specific mineral systems, and an effective performance across various pH conditions [20, 21].

The recent studies have provided further insights into the complexities of particle interactions during flotation. Nowosielska et al. (2022) investigated the interactions between coarse and fine particles of galena and quartz during flotation in the NaCl solutions [22]. Their research work revealed that the presence of fine particles can significantly impact the flotation behavior of coarse particles. In the saline environments, they observed that fine particles sometimes adhered to coarse particles, altering their surface properties, and consequently, affecting the

separation efficiency. This work highlights the importance of considering particle interactions across different size ranges when optimizing the flotation processes for coarse particles.

Complementing this research work, Zhou et al. (2022) focused specifically on how the particle size influences the flotation separation of kaolinite and quartz [23]. Their study demonstrated that particle size had a significant impact on the flotation efficiency. They identified optimal size ranges for separating these minerals, and provided insights into the mechanisms by which the particle size affects the flotation process. This work emphasizes the need for tailored approaches when dealing with different particle size distributions in the flotation systems, particularly when aiming to improve the coarse particle recovery.

This research work explored the synergy between the microbubble technology and the cationic collector environment created by DDA, specifically targeting coarse particle flotation. This combination introduces a unique flotation environment that has not been extensively studied. The interaction between microbubbles and the cationic environment is expected to significantly influence the flotation process, particularly regarding coarse particles [13]. This interaction may alter the microbubble stability, surface charge, and the dynamics of bubble-particle interactions in the previously unobserved ways. Moreover, the complex system resulting from the interplay of the cationic environment, microbubbles, and operational parameters—such as impeller speed, froth thickness, percentage of fine particles, and pulp density—presents a multi-faceted research challenge. Understanding these interactions is essential for optimizing coarse particle flotation, and represents a significant knowledge gap in the field [5].

Our study aims to systematically investigate these factors, providing a comprehensive understanding of this flotation system, which has the potential to redefine approaches to coarse particle flotation. This research work investigates the behaviour of microbubbles in a cationic collector environment, focusing on the mechanisms of hydrodynamic interactions with bubble particles and optimizing coarse particle recovery. By addressing these challenges, the study enhances the understanding of the complex microbubble-assisted flotation systems, with implications for improving recovery rates and energy efficiency.

2. Materials and Methods

2.1. Sample and reagents

A high-purity quartz sample (approximately 98%) was sourced from Adyin, Türkiye. To focus on coarse particle flotation, the fraction below 212 µm was removed via sieving. Additionally, 10 kg of quartz was pulverized to generate fine particles for the study. The sample was purified using the Pashley and Kitchener method: the specimen underwent three successive treatments with a 37% hydrochloric acid (HCl), each lasting 120 minutes, followed by four rinses with distilled water. Subsequently, the sample was immersed in 30% sodium hydroxide (NaOH) at 60 °C for one minute. The purified quartz was then desiccated in an oven at 110 °C overnight. All experiments were conducted using tap water with a pH of 7.74. Post-preparation, the quartz particles were subjected to chemical and mineralogical analyses using X-Ray Fluorescence (XRF) and an X-Ray Diffraction (XRD) spectrometry. Dodecylamine was employed as the cationic collector for quartz in the flotation experiments.

2.2. Flotation experiments

This work utilized a self-aerated Denver flotation machine with a D12 size. The flotation process occurred in a 1.2-litre cell for 4 minutes at room temperature. Raising the impeller velocity led to higher airflow rates, generating larger bubbles [24]. Air suction rate into a self-aeration Denver laboratory flotation cell was measured at various impeller speeds. An airflow meter was connected to the air-controlled valve of the flotation machine to quantify the air flow rate. High-resolution images of the flotation cell were captured to determine the average bubble size at different impeller speeds. These images were then analyzed using the ImageJ software.

The factors that significantly impact the result will be optimized for every process, and those with little to no impact must be removed. The screening process tried to identify the elements significantly affecting the outcome by concentrating primarily on the ambiguous (uncertain) components. Then the optimization method modelled the consequences of these elements. In this work, all experiments have been performed at a pH of 8.5. The amine molecules and the amine ions coexisted in the slurry solution throughout the flotation of minerals with DDA, but their concentrations differed, and the pH of the solution varied substantially. Most of the solutions with strong alkalinity were made up of amine molecules, whose solubility was substantially lower than the amine ions. Where the system's surface

energy increased, the system's surface activity decreased, the repulsive force between hydrophilic groups increased, and the H^+ concentration grew with a firm acidity. As a result, the DDA performed better in the weak acid or weak base conditions, consistent with the Figure 2's findings [25].

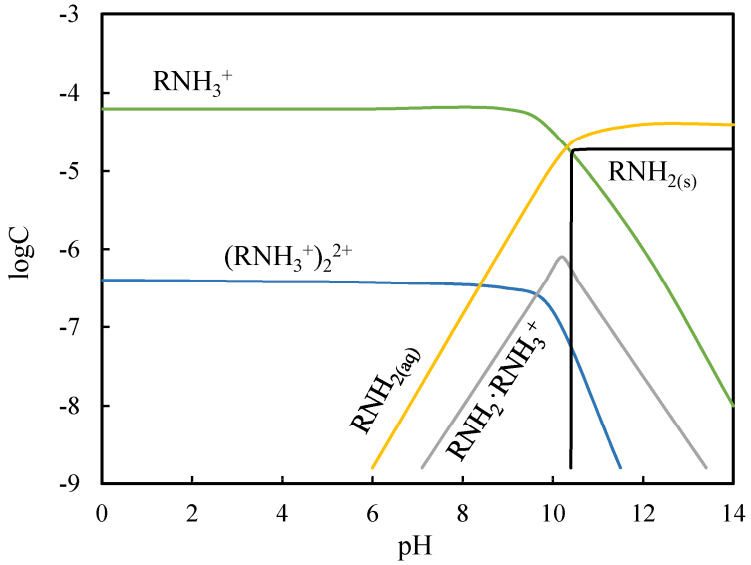

Figure 2. The species distribution chart of dodecylamine (DDA) as a function of pH [26].

2.3. Screening and characterization

Screening and characterization assessments were conducted to investigate the impacts and interplays of MIBC, fine particles, pulp density, and froth thickness under the following circumstances: DDA of 0.1 mmol/L and 950 rpm impeller speed to distinguish the vital parameters from the unknown or dubious parameters. The depth was measured using a calibrated ruler attached to the side of the flotation cell. Before each experiment, the weir was adjusted to achieve the desired froth depth of either 1 cm or 3 cm, and this depth was maintained throughout the flotation process. Whose operational parameters have been delineated in an earlier research work, as displayed in Table 1; flotation tests (20 trials) were performed utilizing a two-level factorial design encompassing five central points.

Table 1. The two-level factorial design parameters for screening experiments.

Factors	Description	Unit	-1	+1
A	MIBC	mmol/L	0.1	1
B	Fine particles	%	0	20
C	Pulp concentration	%	10	40
D	Froth depth	cm	1	3

2.4. Optimization

A six-factor, three-level Box-Behnken experimental design (92 runs) was used to analyze and optimize coarse particles. One element is category, and five are numerical. The studies performed to determine the optimum effects and interactions of DDA, MIBC, impeller speed, pulp concentration, fine particles, and microbubbles are shown in Table 2.

Table 2. The Box-Behnken response surface design parameters for the optimization experiments.

Factors	Description	Unit	-1	0	+1
A	DDA	mmol/L	0.5	2.75	5
B	MIBC	mmol/L	0.1	0.55	1
C	Impeller speed	rpm	700	900	1200
D	Pulp concentration	%	10	25	40
E	Fine particles	%	0	10	20
F	Microbubbles		Absent		Present

All investigations employed randomization to prevent prejudice, and mitigate the influence of unforeseen disparities in the outcomes. An analysis of variance (ANOVA) was utilized to scrutinize the outcomes, and evaluate the interplays among the procedural variables. Five additional confirmatory tests were then run to ensure the optimal outcome of the statistical experimental design.

2.5. Microbubbles generator

Ultrasonic waves, aqueous solvent blends, microfluidics, electrochemical processes, pressure reduction, and temperature adjustments are the technologically viable techniques for producing micro- and nano-bubbles; however, only a few have been created explicitly for the flotation systems. According to Nazari and Hassanzadeh (2020), it includes MicroGas (MG), dissolved air flotation (DAF), Hydrodynamic Cavitation (HC), and a two-phase Centrifugal Multiphase Pump (CMP) [13]. A microbubble generator is seen in Figure 3, and was provided by the China's Dongguan Technology Co., Ltd. A direct-connected motor serves as the pump body for the gas-liquid mixing. An air compressor or atmospheric ejector is not necessary because the suction inlet of the gas-liquid mixing pump utilizes negative pressure to pull in gas. The gas and liquid are entirely dissolved because of the pressure-controlled mixing in the pump.

Consequently, producing a greatly dissolved liquid without needing a substantial reaction tower or a pressurized gas reservoir is possible. The centrifugal pump used to create microbubbles has a gas-to-liquid ratio of 1:9, and a flow rate of 20 L/min. According to the manufacturer's specifications, this device produces microbubbles ranging from 20 to 30 µm.

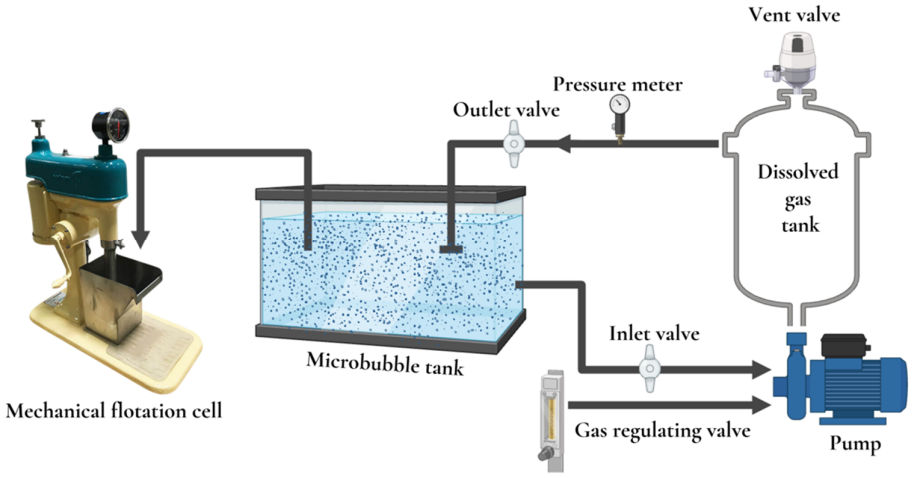

Figure 3. Schematic diagram of the microbubble generator used in the study.

3. Results and Discussion

3.1. Sample characterization

Initial particle size analysis using a Malvern Mastersizer revealed a D50 of 276 µm for the raw sample. Following the removal of sub-212 µm particles, subsequent size measurement yielded a D50 of 495 µm, as illustrated in Figure 4. This significant increase in median particle size confirms the successful isolation of the coarse fraction for the flotation studies. The fine particle fraction, generated through grinding, exhibited a D50 of 40.2 µm, providing a suitable size distribution for investigating the impact of fines on coarse particle flotation. The results of the XRF and XRD analyses, presented in Table 3 and Figure 5, respectively, provide a comprehensive information on the prepared quartz sample's chemical composition and crystalline structure, confirming its high purity and suitability for the flotation experiments.

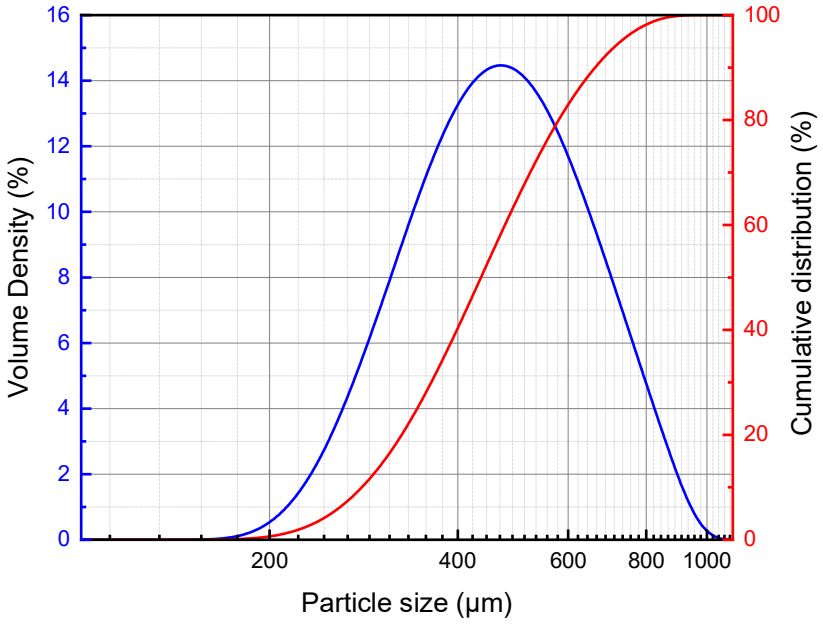

Figure 4. Particle size distribution of the quartz sample after removal of particles smaller than 212 µm.

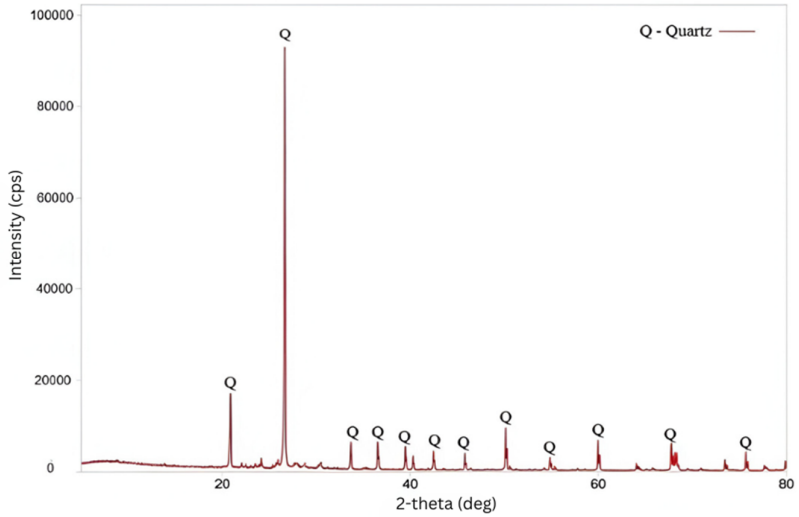

Figure 5. The XRD pattern of the quartz sample.

Table 3. The XRF analysis results of the quartz sample used in the flotation experiments.

Component	SiO_2	Al_2O_3	Na_2O	P_2O_5	TiO_2	MnO	MgO	K_2O	Fe_2O_3	CaO	A.Za
Content (wt.%)	97.7	0.6	0.3	< 0.1	< 0.1	< 0.1	0.1	< 0.1	0.4	0.2	0.3

3.2. Air flow rate and bubble size measurement

The self-aeration mechanism in the Denver cells relies on the low-pressure zone created by the rotating impeller. As the impeller speed increases, it generates a stronger vortex, and a more pronounced low-pressure area at its center. This enhanced suction effect draws more air through the standpipe, resulting in the observed linear increase in air flow rate from about 0.18 L/min at 700 rpm to 0.65 L/min at 1200 rpm, as shown in Figure 6. This phenomenon aligns with the findings of Gorain et al. (1997), who studied gas dispersion characteristics in self-aerating flotation machines [27].

Concurrently, the bubble grows from approximately 0.12 mm to 0.6 mm over the same speed range. This increase in the bubble size can be attributed to several factors. The higher turbulence at increased impeller speeds leads to a more frequent

bubble coalescence, as Jameson et al. (2007) described in their work on bubble breakup and coalescence in the flotation environments. Additionally, the greater volume of air introduced into the cell allows larger bubbles to form, and persist [28].

3.3. Screening and characterization

The half-normal and perturbation graphs in Figure 7 show that the most significant impacts were caused by the fine particles (B), MIBC (A), and pulp concentration (C). Froth depth (D) did not significantly impact the recovery. Froth depth will not be included in the optimization process since only crucial variables and their interactions are required. A decrease in the froth depth enhances the flotation of the coarse particle by reducing the residence duration, which is a function of the froth depth. On the other hand, overall recovery slightly increased when the froth depth was decreased. This is due to the increased recovery of gangue via entrainment, which would contaminate the concentrate [29, 30]. Pure quartz was utilized in this investigation in a 1.2-L flotation cell; therefore, its effect on the recovery of the coarse particle was only slightly noticeable in contrast to the alternative factors.

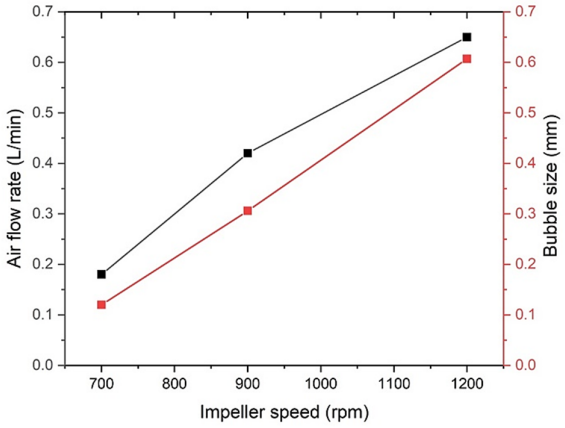

Figure 6. Effect of impeller speed on the air flow rate and bubble size in a self-aerating Denver flotation cell.

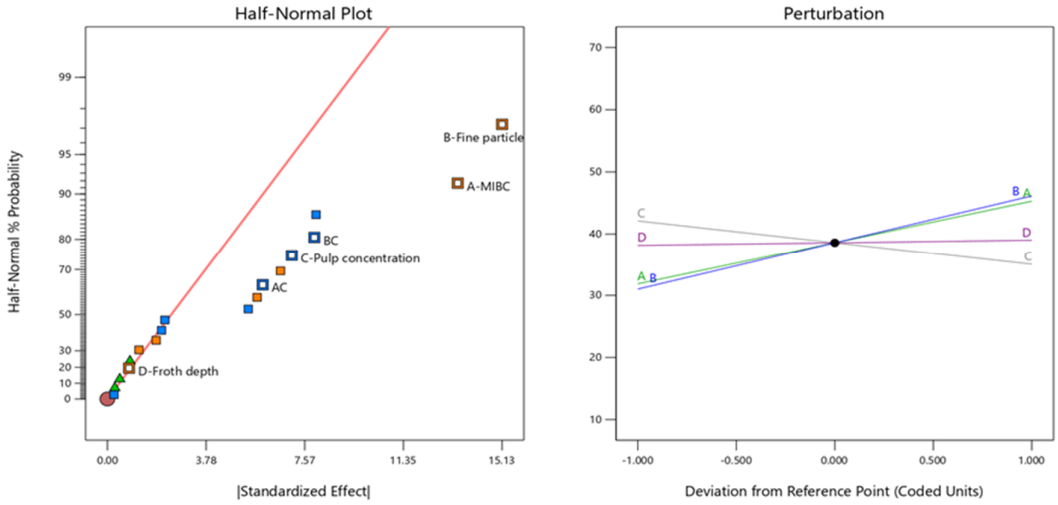

Figure 7. Half-normal and perturbation plots showing the relative importance of MIBC (A), fine particles (B), pulp concentration (C), and froth depth (D) on the flotation recovery.

3.4. Analysis of variance (ANOVA)

The analysis of variance (ANOVA) for the model of flotation recovery (Table 4) yields several statistically significant observations into the process of dynamics. The model demonstrates a high statistical significance ($p < 0.0001$, $F = 61.87$), indicating its robust capacity to elucidate the variance in recovery. The probability of this F-value occurring due to noise is negligible (0.01%), underscoring the model's reliability, and statistical power. Among the individual factors, the dodecylamine (DDA) concentration (A), impeller speed (C), fine particle content (E), and microbubble presence (F) emerge as the most statistically significant ($p < 0.0001$). The DDA concentration and the impeller speed exhibit particularly substantial effects, as evidenced by their exceptionally high F-values (398.11 and 657.84, respectively). These results strongly suggest that these parameters exert the most profound influence on flotation recovery efficiency. As indicated in the p-value column, MIBC (B) and some interactions have values greater

than 0.05, but they were kept in the model to maintain the hierarchy.

The ANOVA also reveals several significant factors that interact with each other. Notable among these are the interactions between the DDA concentration and the impeller speed (AC), the impeller speed and the pulp concentration (CD), DDA and fine particles (AE), and fine particles and microbubbles (EF). The statistical significance of these interactions indicates complex, multi-faceted relationships between these factors in the modulating recovery, highlighting the intricate nature of the flotation process. Interestingly, the model incorporates significant quadratic terms (A^2, C^2, E^2), indicative of the non-linear relationships between these factors and recovery. This non-linearity is particularly pronounced for the DDA concentration and the impeller speed, suggesting that their effects on recovery are not monotonic, and likely exhibit optimal ranges within the experimental domain. The presence of significant higher-order interactions such as the three-way interaction ADF (DDA, pulp concentration, and microbubbles), and the quadratic interactions between A^2F and C^2F, further emphasizes the complexity of the flotation system. These higher-order interactions suggest that the effects of certain factors on the recovery are contingent upon the levels of multiple other factors simultaneously, necessitating a nuanced approach to process optimization.

Notably, the concentration of Methyl IsoButyl Carbinol (MIBC) (B) does not exhibit statistical significance in this model ($p = 0.3373$). Given the ubiquitous use of MIBC in the flotation processes, this unexpected finding suggests that in this specific system, MIBC plays a subordinate role compared with other factors. While the model demonstrates a strong overall significance, it is pertinent to note that the lack of fit ($p = 0.0691$) approaches statistical significance. Although not significant at the conventional $\alpha = 0.05$ level, this borderline value indicates that there may be aspects of the process that the model does not fully capture. This suggests the potential for further refinement or the inclusion of additional factors to model the flotation dynamics more comprehensively.

Table 4. Analysis of variance (ANOVA) for the model of flotation recovery.

Source	Sum of Squares	df	Mean Square	F-value	p-value	
Model	262.82	22	11.95	61.87	< 0.0001	Significant
A-DDA	76.86	1	76.86	398.11	< 0.0001	
B-MIBC	0.1802	1	0.1802	0.9336	0.3373	
C-Impeller speed	127.01	1	127.01	657.84	< 0.0001	
D-Pulp concentration	1.85	1	1.85	9.60	0.0028	
E- Fine particles	4.08	1	4.08	21.11	< 0.0001	
F-Microbubbles	17.18	1	17.18	88.96	< 0.0001	
AC	2.18	1	2.18	11.31	0.0013	
AD	0.0044	1	0.0044	0.0228	0.8804	
AE	1.33	1	1.33	6.90	0.0106	
AF	0.0176	1	0.0176	0.0911	0.7637	
BC	0.1952	1	0.1952	1.01	0.3182	
CD	4.79	1	4.79	24.83	< 0.0001	
CE	1.01	1	1.01	5.22	0.0254	
CF	0.5133	1	0.5133	2.66	0.1076	
DF	0.0012	1	0.0012	0.0062	0.9375	
EF	1.31	1	1.31	6.78	0.0113	
A^2	12.52	1	12.52	64.82	< 0.0001	
C^2	6.27	1	6.27	32.49	< 0.0001	
E^2	1.99	1	1.99	10.31	0.0020	
ADF	0.8388	1	0.8388	4.34	0.0408	
A^2F	3.84	1	3.84	19.89	< 0.0001	
C^2F	2.23	1	2.23	11.55	0.0011	
Residual	13.32	69	0.1931			
Lack of Fit	12.43	59	0.2108	2.38	0.0691	not significant
Pure Error	0.8872	10	0.0887			
Cor Total	276.14	91				

3.5. Modeling

The quadratic models are presented utilizing a coded factor to demonstrate the application of experimental models in exploring the relationship between the process variables and the flotation recovery outcomes:

Recovery = 6.01 + 1.55 A + 0.0751 B + 1.99 C + 0.2407 D – 0.357 E + 0.6488 F - 0.0774 CD + 0.5225 AC + 0.0235 AD - 0.4081 AE + 0.0234 AF – 0.2424 BC - 0.3550 CE + 0.1266 CF + 0.0061 DF + 0.2022 EF – 0.7957 A^2 – 0.5634 C^2 + 0.3174 E^2 + 0.324 ADF - 0.4339 A^2F - 0.3306 C^2F

For the specific values of each element, the reaction may be predicted using the coded factor equation. The coefficient's positive value suggests synergistic benefits, whereas its negative sign implies the antagonistic effects. The bigger factor coefficients suggest that a factor has a more profound impact on the flotation performance. The constant value of 6.01 remains consistent across the operational parameters. The linear factor E, and the quadratic terms A^2 and C^2, and the interaction components AE, BC, CD, CE, A^2F, and C^2F exhibit a detrimental impact on recovery, suggesting a decline in grade with their increased values. Conversely, A, B, C, D, F, AC, AD, AF, CF, DF, EF, and ADF positively affect the outcome, signifying an enhancement in the response with a higher outcome of these factors.

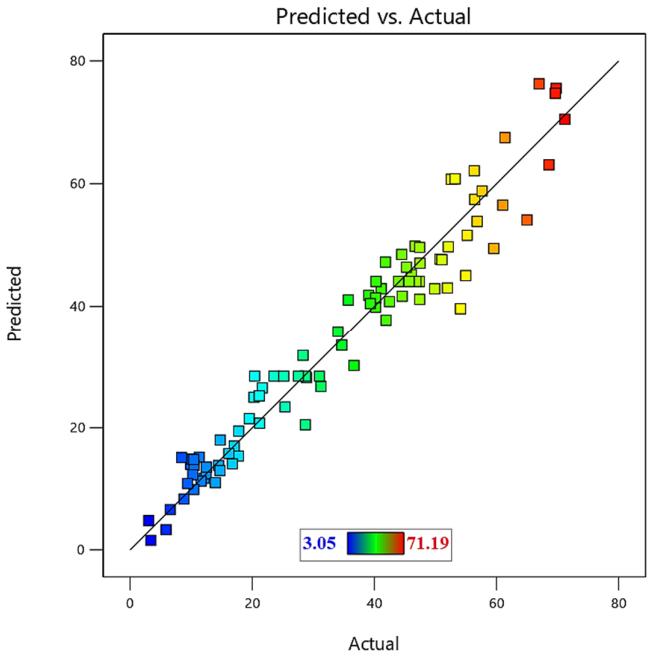

Figure 8. Correlation between the predicted and observed experimental recovery values.

The statistical assessment for lack of fit confirms the adequacy of the provided equation as a predictive model for the flotation recovery. The signal-to-noise ratio stands at 34.3638, displaying the requisite precision level. This ratio surpasses 4, validating its suitability for navigating the design space using the model. Furthermore, the incorporation of the Box-Behnken design data into the model allowed for the assessment of the recovery model viability, indicated by the R^2 correlation coefficient value of 0.9518. The close association between the experimental and anticipated outcomes is evidenced by this data, further supported by the variance in the mean calculated using the adjusted R^2, which stands at 0.9364. The proximity of R^2 and adjusted R^2, both within 0.20 of each other, highlights the close alignment between the recovered and predicted data. A successful model is characterized by the results closely mirroring predicted and actual values, as reflected in the model's low standard deviation of 0.4394. Additionally, the relationship plots between the actual data and the predicted recovery responses are depicted in Figure 8; it reveal a strong linear resemblance, suggesting that the reaction can be reliably anticipated using the modeling equations derived from the individual elements.

3.6. Perturbation analysis

Perturbation was utilized to elucidate the primary effects of the independent variables and their interplay on the recovery. Figure 9(a-b) delineate the impacts of DDA (A), MIBC (B), impeller speed (C), pulp concentration (D), and fine particles (E) on the recovery, both in the absence and presence of microbubbles. In Figure 9(a), it is evident that DDA (A) exerts the most significant influence on recovery in the absence of microbubbles, followed by the

impeller speed (C) and fine particles (E), whereas the MIBC (B) and pulp concentration (D) wield a little influence. Conversely, Figure 9(b) depicts a similar effect of the variables in the existence of microbubbles, albeit with an average total recovery increase of 15%. This augmentation can be attributed to the heightened likelihood of particle-bubble attachment facilitated by microbubbles, commonly known as the "bridge effect" or "secondary collector role." This occurs as numerous ultra-fine bubbles on mineral surfaces amalgamate with coarse bubbles [13]. The DDA (A) concentration demonstrates a pronounced non-linear effect, with a steep positive slope at lower concentrations that gradually plateaus at higher levels, indicating diminishing returns and suggesting an optimal dosage range. The impeller speed (C) exhibits an S-shaped non-linear relationship, implying a "sweet spot", where the recovery improvement is maximized, likely due to the optimal bubble-particle collision dynamics. Fine particles (E) show a non-linear negative impact on the recovery, with a steeper decline at lower concentrations that bhemes less pronounced at higher levels, suggesting that their detrimental effect is most significant upon initial introduction but may stabilize as their concentration increases.

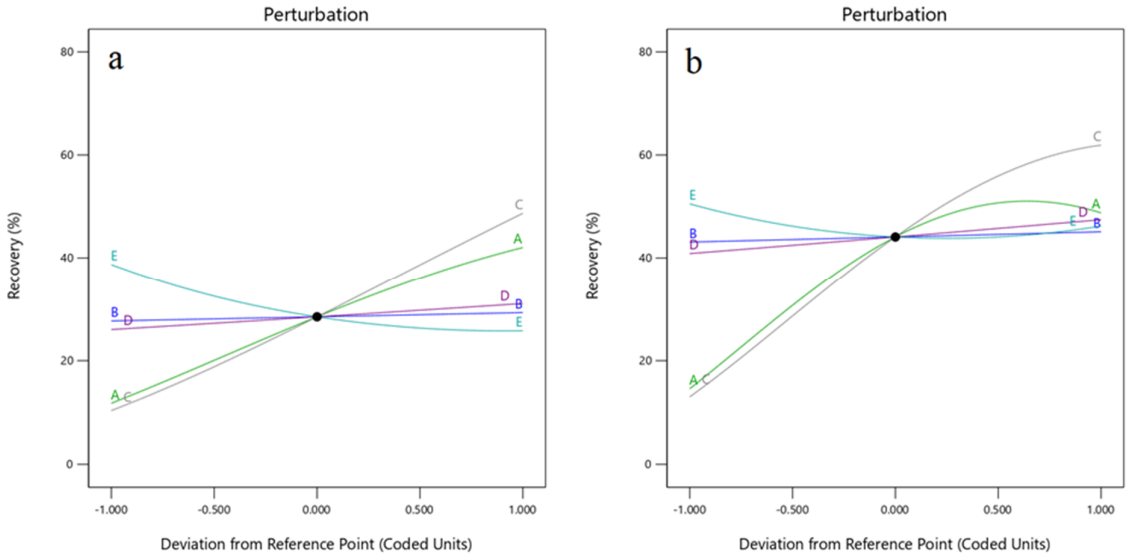

Figure 9. Recovery perturbation diagrams illustrating the impacts of DDA (A), MIBC (B), impeller speed (C), pulp concentration (D), and fine particles (E) on flotation recovery; (a) in the absence of microbubbles and (b) under microbubble conditions.

3.7. Synergistic Effects of Parameters and Microbubbles

3.7.1. Interaction between DDA concentration and microbubbles

The interaction between the dodecylamine (DDA) concentration and microbubbles, as illustrated in Figure 10, reveals a complex relationship. At low DDA concentrations, the recovery was significantly higher than the condition without microbubbles, exhibiting an increase of up to 20%. This observation aligns with the findings of Ahmadi et al. (2014), who reported that microbubbles could enhance the flotation performance, particularly when there is a limited collector coverage [31]. As the DDA concentration increases, the recovery continues to rise, albeit at a diminishing rate, with the curve beginning to plateau. This shape indicates a "saturation effect", wherein the benefits of microbubbles become less pronounced at higher DDA dosages. The diminishing impact of microbubbles at higher DDA concentrations could be attributed to the particle surfaces becoming sufficiently hydrophobic, thereby reducing the relative impact of the additional surface area provided by microbubbles.

3.7.2. Effect of MIBC concentration with microbubbles

Figure 11 depicts the effect of varying concentrations of methyl isobutyl carbinol (MIBC) with and without microbubbles. At low MIBC levels, the recovery is significantly higher when microbubbles are present, suggesting their important role in enhancing froth performance. This indicates that microbubbles can partially compensate for inadequate frother coverage by contributing to the froth stability, and increasing bubble surface area. As the MIBC concentration rises, recovery shows a

modest improvement; however, the benefits conferred by microbubbles diminish. This may reflect a "complementary effect", where the roles of MIBC and microbubbles in the froth stabilization and bubble-particle attachment begin to overlap. At elevated MIBC concentrations, excessive frother dosages appear to negate the advantages of microbubbles, potentially due to over-stabilization of the froth, disruption of bubble-particle interactions, or alterations in the microbubble size distribution or stability under high frother conditions.

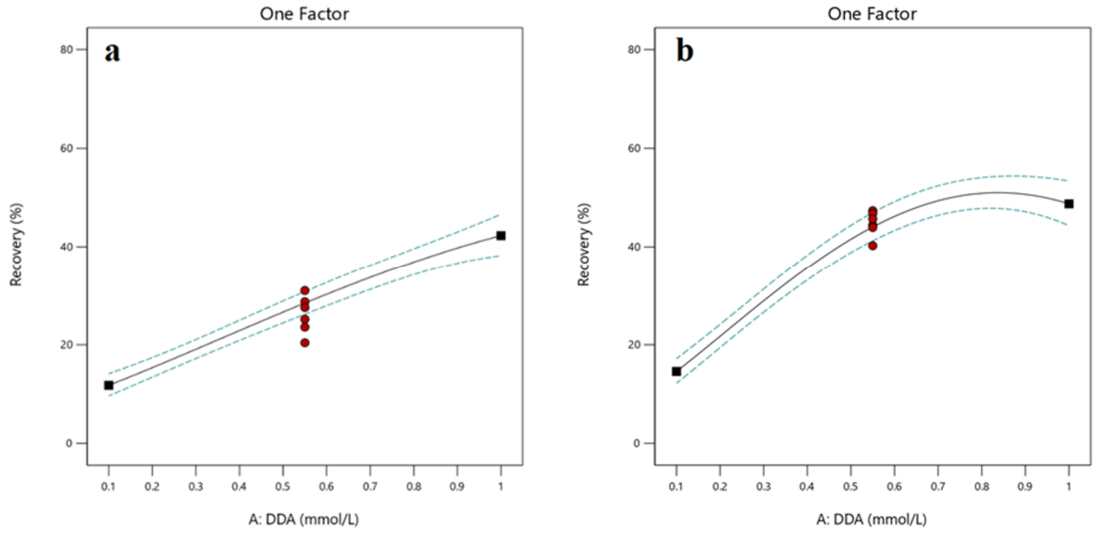

Figure 10. Effect of the dodecylamine (DDA) concentration on the flotation recovery: (a) without microbubbles, (b) with microbubbles.

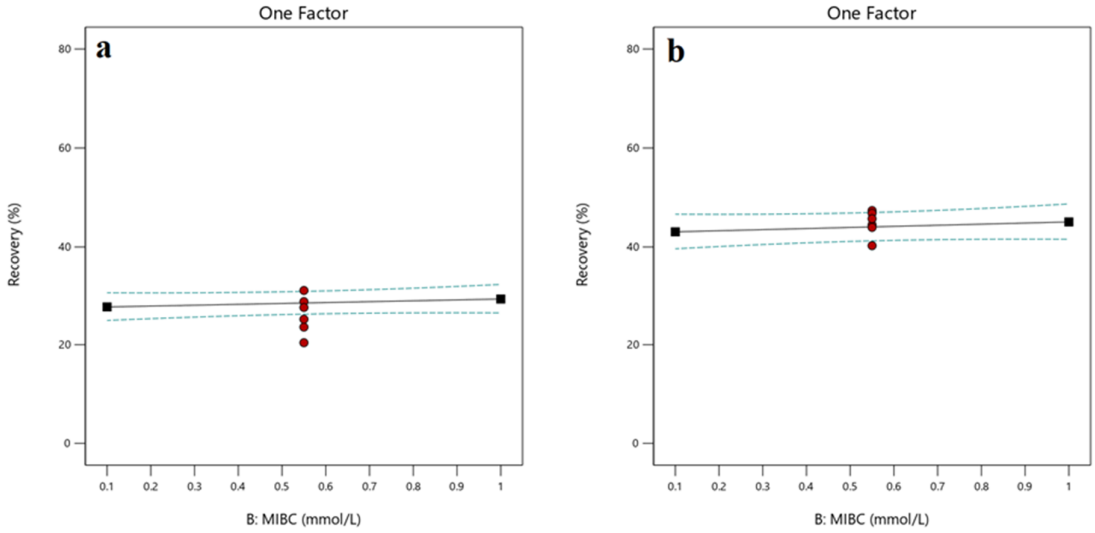

Figure 11. Influence of the MIBC concentration on the flotation recovery: (a) without microbubbles, (b) with microbubbles.

3.7.3. Impact of impeller speed with microbubbles

Figure 12 illustrates the impact of varying impeller speeds on the recovery in the presence and absence of microbubbles. At low impeller speeds, the recovery is markedly higher in the presence of microbubbles, as seen in Figure 12(b), compared to Figure 12(a). This enhancement is likely attributable to the microbubbles' increased surface area-to-volume ratio, which improves the probability of bubble-particle attachment. As impeller speed increases to moderate levels; the recovery improves in both cases. However, the recovery enhancement due to microbubbles remains pronounced, indicating that microbubbles continue to confer an advantage even as turbulence rises. The steeper recovery slope

in the presence of microbubbles suggests that they enhance the system sensitivity to changes in the hydrodynamic conditions by improving the suspension of coarse particles. At high impeller speeds, recovery continues to increase in both scenarios, though the rate of improvement slows, particularly with microbubbles. This plateau may be due to a saturation in the collision efficiency or adverse effects of excessive turbulence. Nonetheless, the persistent recovery gap between the two conditions at high speeds demonstrates that microbubbles retain their beneficial effect even under high-shear environments, contrary to the expectations that turbulence would destroy them.

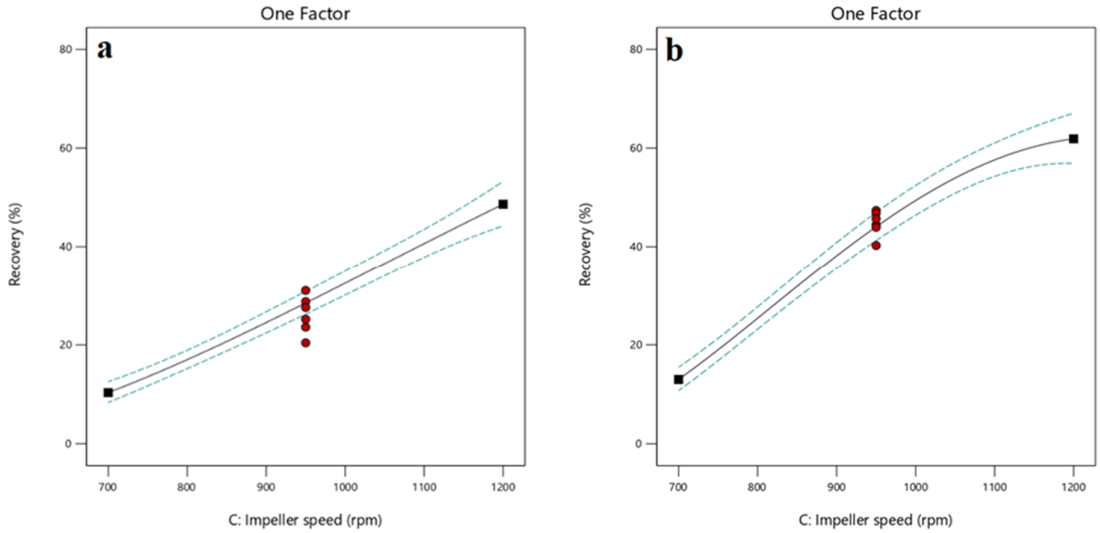

Figure 12. Impact of the impeller speed on the flotation recovery: (a) without microbubbles, (b) with microbubbles.

3.7.4. Effect of pulp concentration with microbubbles

Figure 13 illustrates the effect of pulp concentration on the recovery in systems with and without microbubbles. The recovery with microbubbles is slightly higher than without at low pulp concentrations, suggesting that the benefit of microbubbles at low pulp densities is limited by the relatively low probability of bubble-particle collisions. As the pulp concentration increases, recovery improves in both conditions, though the recovery gap between systems with and without microbubbles widens. This trend implies a synergistic effect, in which the increased particle density enhances the effectiveness of microbubbles, likely due to higher collision frequencies, and more efficient utilization of the microbubble surface area.

3.7.5. Influence of fine particle content with microbubbles

Figure 14 demonstrates the effect of the fine particle content on the recovery in the presence and absence of microbubbles, revealing interesting interactions between fine particles and microbubbles. At a low fine particle content, the recovery in the presence of microbubbles is approximately 15% higher than in their absence. This improvement is likely due to the increased probability of bubble-particle collisions and microbubbles' "bridging" effect. As the fine particle content increases, the recovery decreases in both conditions, though the recovery gap between the systems with and without microbubbles widens. This suggests that the positive effect of microbubbles diminishes as fine particles compete with coarse particles for the attachment sites. In the systems without microbubbles, excessive fines may lead to slime coatings or over-consumption of collectors, further diminishing the recovery efficiency.

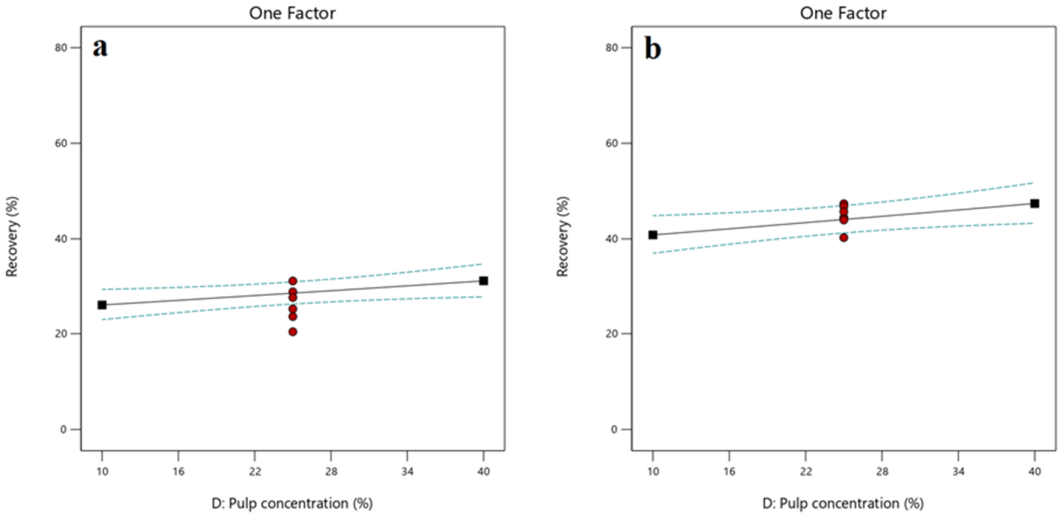

Figure 13. Effect of the pulp concentration on the flotation recovery: (a) without microbubbles, (b) with microbubbles.

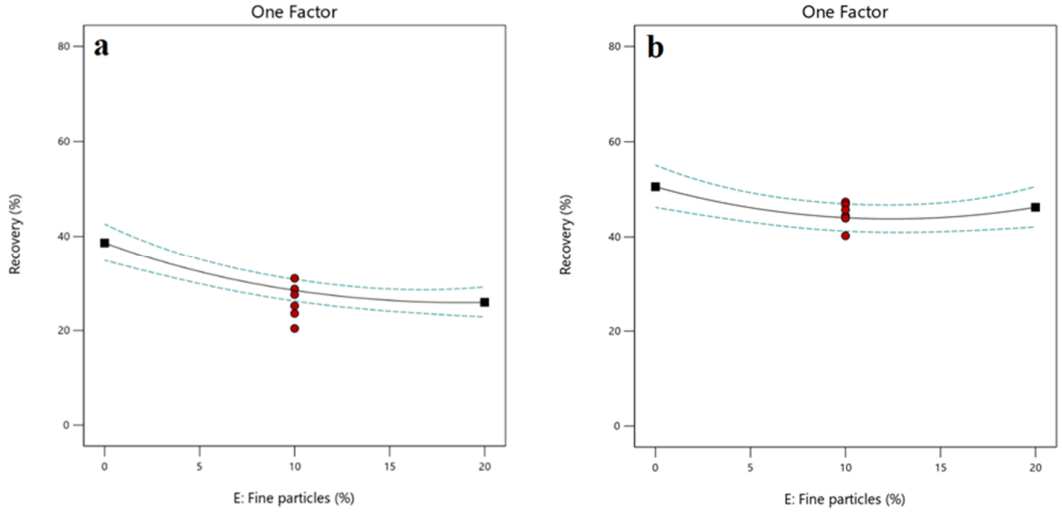

Figure 14. Influence of the fine particle content on the flotation recovery: (a) without microbubbles, (b) with microbubbles.

3.8. Collective impact of factors

The reciprocal repercussions of every duo of autonomous factors, at the average level of the other autonomous variables, on the reliant variable of recovery responses were delineated through the three-dimensional response surface graphs.

In both scenarios, iteh and without microbubbles, Figure 15 shows the cases the interactive influence of DDA (A) and MIBC (B) at the mean level of impeller speed (C), pulp concentration (D), and fine particles (E). In the absence of microbubbles, DDA exhibits a dominant effect, while MIBC's impact on recovery remains relatively weak, peaking at 40% (Figure 15(a)). Conversely, when microbubbles are introduced, recovery escalates to 50% (Figure 15(b)). Regardless of the presence of microbubbles, DDA significantly influences the recovery more than MIBC. Augmenting the collector (organic surfactant) quantity diminishes the pulp surface tension, aligning with the Gibbs adsorption equation [32]. It's widely acknowledged that a surfactant addition lowers surface tension, and reduces bubble size, mirroring the effects of a frother [33]. Wiese et al. (2010) cautioned against excessive frother usage, as it can destabilize froth, resulting in the diminished recovery. An overabundant frother can engender an excessively stable froth hindering mineral particle capture in the concentrate, relegating them to the tailings. The overall recovery rates are enhanced with the microbubble introduction due to their

extensive surface area, facilitating hydrophobic particle attachment, bolstering the likelihood of particle-bubble collision and adherence [3, 35, 36]. The collector impact supersedes that of frother in coarse particle flotation, a phenomenon elucidated by microbubble utilization. Microbubbles foster a uniform distribution and efficacious interaction between the bubbles and hydrophobic particles. Nazari et al. (2018) found that in using microbubbles in flotation, the collector presence can offset the absence of a frother [16].

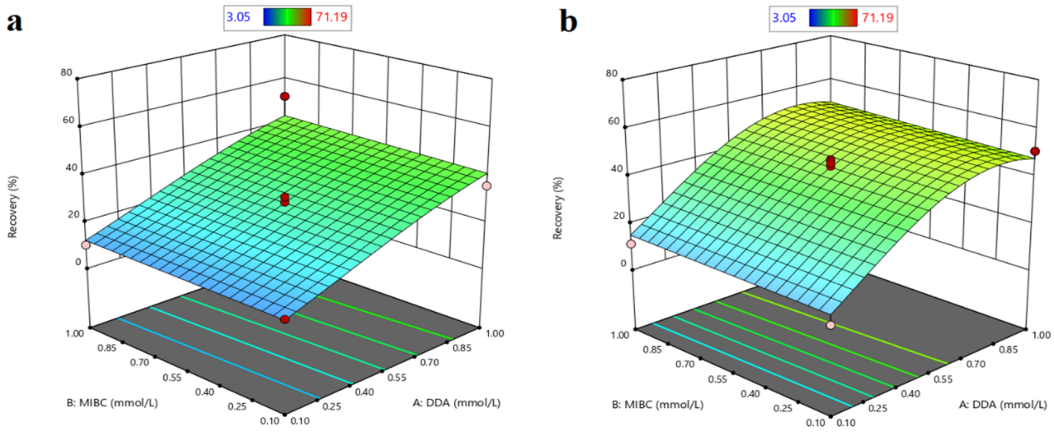

Figure 15. 3D response surface plots showing the interactive the effects of DDA and MIBC concentrations on the flotation recovery at mean levels of other parameters: (a) without microbubbles and (b) with microbubbles.

At the average levels of MIBC (B), pulp concentration (D), and fine particles (E), both with and without microbubbles, Figure 16 displays the combined effect of DDA (A) and impeller speed (C). The recovery reached 71% when both the impeller speed and DDA were at their peak, as depicted in Figure 16(a). Figure 16(b) shows a similar outcome with no significant variation. At lower impeller speeds, the likelihood of collisions diminishes due to insufficient energy to stir the heavier particles, leading to their settling in the cell and affecting recovery [37]. Conversely, at higher impeller speeds, the chances of collision and detachment increase, with the flotation recovery largely relying on the attachment between particles and bubbles [38]. Particle-bubble detachment becomes more likely as the surface hydrophobicity decreases, which reduces the collector coverage [39].

Additionally, particle-bubble conglomerates in the pulp are susceptible to breakup in turbulent hydrodynamic environments when the impeller speeds exceed 1300 rpm. The agitation intensity inversely affects the bubble size: higher speeds produce smaller bubbles, increasing the likelihood of collisions [38, 40]. The combined presence of smaller bubbles and microbubbles at high speeds boosts the collision rates, and improves the recovery. Therefore, the observed results can be attributed to the strong adsorption of the collector on the mineral surface.

Figure 17 depicts the interaction between the DDA (A) and pulp concentration (D) at the average levels of other variables, both with and without microbubbles. In the absence of microbubbles (Figure 17(a)), the pulp concentration exhibited a minimal influence on the recovery; nevertheless, the recovery improved proportionately to 40% when DDA was increased. The pulp concentration started affecting the recovery when DDA was more significant than 0.6 mmol/L in the presence of microbubbles, and recovery increased as the pulp concentration increased, reaching nearly 60%, as shown in Figure 17(b). This result occurred because a higher pulp density can increase the likelihood of particle-bubble collisions, facilitating the attachment of additional mineral particles to air bubbles, and their transfer to the froth phase [29]. The introduction of microbubbles enhances the effective volume of the flotation pulp. Due to their larger surface area compared to the bigger bubbles, microbubbles increase the pulp's void fraction, effectively reducing the bulk density of the pulp. Microbubbles could have increased the likelihood of particle-bubble adhesion and angle of contact due to the recognized "bridge effect" or secondary collecting function, where numerous ultrafine bubbles on the mineral surfaces merge with regular bubbles at an adequate collector concentration [13].

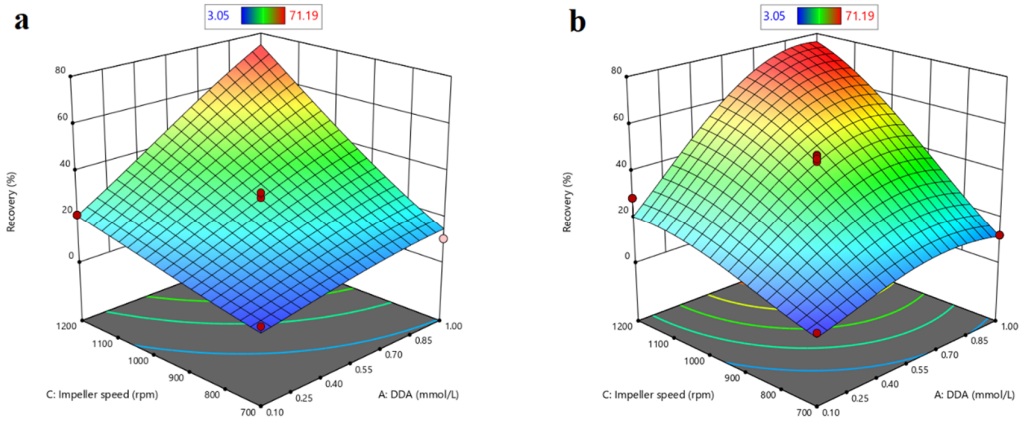

Figure 16. 3D response surface plots depicting the combined effect of the DDA concentration and impeller speed on the flotation recovery at mean levels of other parameters: (a) without microbubbles and (b) with microbubbles.

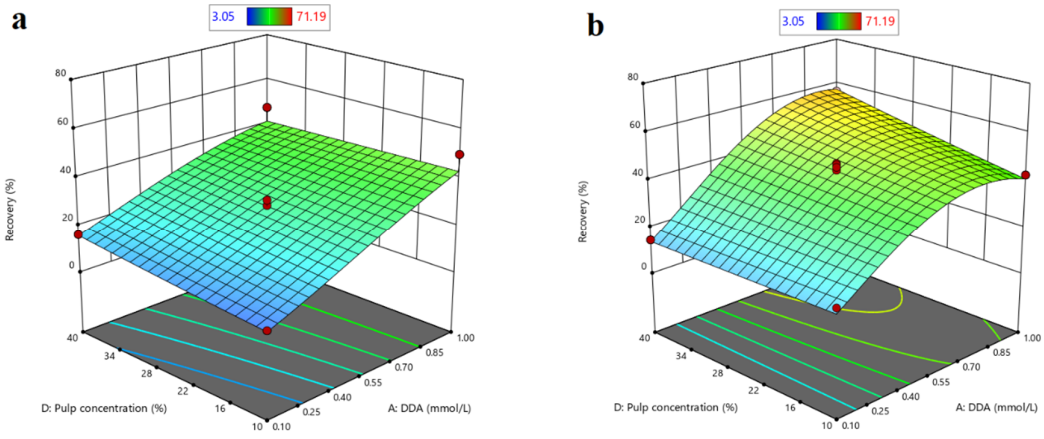

Figure 17. 3D response surface plots illustrating the interaction between the DDA concentration and pulp concentration on the flotation recovery at mean levels of other parameters: (a) without microbubbles and (b) with microbubbles.

The interaction between DDA (A) and fine particles (E) is presented in Figure 18 at the mean value of other parameters in both the presence and absence of microbubbles. Increasing the fine particle amounts harm the recovery as they consume huge collectors. This consumption happened due to their high surface area, which requires more DDA to cover them. Furthermore, coarse particles require a more prominent collector convert area than fine particles because of their high density [41, 42]. Hence, the effect of fine particles could be seen in both cases, with and without microbubbles. Although the maximum recovery of 60% in both environments was identical, Figure 18(b) shows that the overall recovery of a vast amount of DDA in the presence of microbubbles is more significant than in their absence, as presented in Figure 18(a). As Rahman et al. (2012) suggested, fine particles must be present in adequate quantities to improve coarse particle flotation [30].

In contrast, their suggestions build upon a cylindrical Perspex column, not mechanical flotation cells, for which their conditions are more likely to be accurate. Several factors including particle size distribution, particle surface characteristics, and flotation conditions may influence the effects of fine particles in coarse particle flotation. By improving the flotation process parameters, it may be possible to improve the efficiency of coarse particle flotation, and reduce the harmful effects of fine particles.

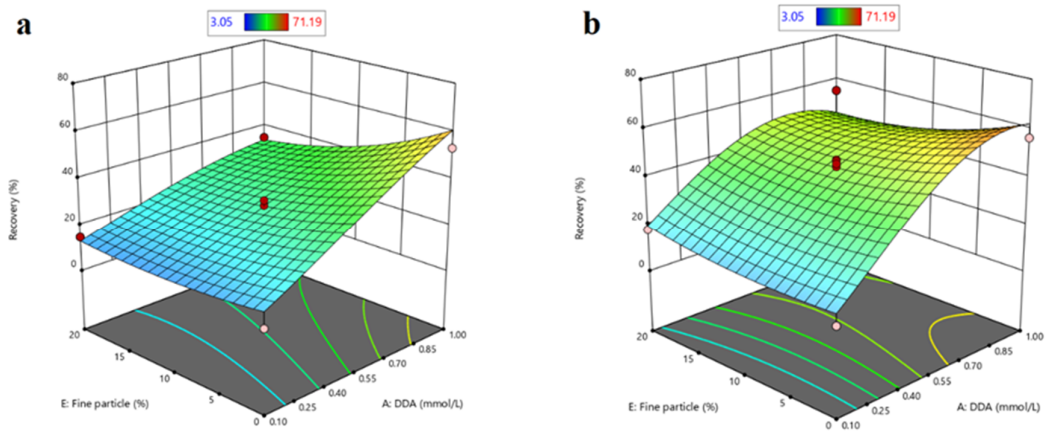

Figure 18. 3D response surface plots showing the interaction between the DDA concentration and fine particle percentage on the flotation recovery at mean levels of other parameters: (a) without microbubbles and (b) with microbubbles.

3.9. Optimization

The experimental design can improve the process conditions by setting the necessary response objectives. The current study aims to maximize and enhance the recovery from coarse particle flotation. The optimal flotation conditions were determined to be 0.988 mmol/L DDA, 0.249 mmol/L MIBC, 1181.851 rpm impeller speed, 27.75% pulp concentration, and 0.08% fine particles in the absence of microbubbles, which produced the most significant recovery of approximately 97.88%. On the other hand, it was found that the ideal flotation conditions in the presence of microbubbles were 0.959 mmol/L DDA, 0.57 mmol/L MIBC, 1199.35 rpm impeller speed, 24.08% pulp concentration, and 0.07% fine particles, which led to a maximum recovery of 99.47%. Five confirmation flotation tests were conducted for each category of microbubbles under ideal circumstances to evaluate the Box-Behnken design, and the optimization results. The mean recovery from these validation experiments fell within the predicted range, and closely matched the predicted values, demonstrating the potential of the suggested model to enhance the flotation performance.

3.10. Comparison with related studies

To contextualize our findings within the broader field of coarse particle flotation research work, we compared our results with three recent studies that also investigated the use of micro or nanobubbles in the quartz flotation. This comparison helps to highlight the unique aspects of our approach, and situate our findings within the current state of knowledge.

Table X presents a comparative analysis of our study with three related works, highlighting the key similarities and differences in approach and findings.

As evident from Table 5, while all studies aimed to improve coarse quartz particle flotation and achieved high recovery rates, there are notable differences in approach and findings. Our study utilized a larger microbubble (20-30 μm) compared to the nanobubbles (< 1 μm) used in the other studies. Additionally, our comprehensive factorial and Box-Behnken design allowed us to optimize the multiple parameters simultaneously, revealing complex interactions that may not have been apparent in more focused studies.

Interestingly, while the other studies emphasized the significant role of nanobubbles in improving the flotation efficiency, our results suggest that microbubbles have a less pronounced impact when other parameters are optimized. This discrepancy could be attributed to the differences in the experimental setups, particle sizes, bubble generation methods, and the range of parameters studied.

Our finding that conventional parameter optimization may be more crucial than the microbubble introduction for enhancing flotation efficiency of larger particles represents a novel contribution to the field. It suggests that the benefits of micro or nanobubbles may be context-dependent, and most significant in the sub-optimal conditions.

Table 5. Presents a comparative analysis of our study with three related works, highlighting the key similarities and differences in approach and findings.

Study	Similarities	Differences
This study (2024)	- Used an amine-based collector (DDA). - Focused on coarse quartz particles. Achieved high recovery rates (> 90%).	- Used microbubbles (20-30 μm). - Comprehensive factorial and Box-Behnken design. - Hydrodynamic condition and chemical environment factors. - Found microbubbles less impactful when other parameters optimized. - Particle size D50 = 495 μm.
Rubio et al. (2024) [43]	- Used an amine-based collector (DDA). - Focused on coarse quartz particles. Achieved high recovery rates (> 90%).	- Used nanobubbles. - One factor at a time (OFAT) design method (no interactions). - Mini-column flotation cell. - Emphasized role of nanobubbles as "seeds" for larger bubbles. - Studied specific size ranges (-20 μm, - 74 + 20 μm and - 150 + 74 μm).
Nazari & Hassanzadeh (2020) [44]	- Used amine-based collector (DDA). - Focused on coarse quartz particles. - Achieved high recovery rates (> 90%).	- Used nanobubbles. - One factor at a time (OFAT) design method (no interactions). - Compared DDA nanobubbles with common frothers. - Emphasized significant improvement with DDA-nanobubbles. - Studied specific size ranges (-425 + 300 μm, −300 + 212 μm and − 212 + 106 μm). - Emphasized bubble size distribution.
Nazari et al. (2020) [45]	- Used nanobubbles. - Focused on coarse quartz particles. - Achieved high recovery rates (> 90%).	- One factor at a time (OFAT) design method (no interactions). - Studied specific size ranges (-425 + 106 μm). - Compared different nanobubble sizes (110, 171, 293 nm).

4. Conclusions

This work has provided valuable insights into optimizing coarse particle flotation using microbubble-assisted flotation in a cationic environment created by dodecylamine (DDA). Our comprehensive investigation of coarse quartz particles (D50 = 495 μm) has revealed several important findings:

1. Combining microbubbles and a cationic collector environment shows promise for enhancing coarse particle flotation, addressing a significant challenge in mineral processing.
2. The DDA concentration and the impeller speed emerged as the most influential factors affecting the recovery rates, highlighting the importance of these parameters in the flotation optimization.
3. While microbubbles increased recovery by an average of 15% under non-optimized conditions, their impact was less pronounced when all parameters were optimized. This outcome suggests that the benefits of microbubbles may be context-dependent, and most significant in the sub-optimal conditions.
4. The optimized flotation conditions achieved remarkably high recovery rates (99.47% with microbubbles and 97.88% without), demonstrating the potential for significant improvements in the coarse particle flotation efficiency through careful parameter optimization.
5. The minimal difference in the recovery rates between optimized conditions with and without microbubbles indicates that the conventional parameter optimization may be more crucial than the microbubble introduction for enhancing the flotation efficiency of larger particles.

This work enhances our understanding of complex flotation systems involving cationic collectors and microbubbles for coarse particles. It challenges the universal benefit of the microbubble technology, suggesting that its effectiveness depends on other operational parameters. The research work has industrial implications, showing the potential for improved mineral processing through the conventional parameter optimization. Future research should explore these findings' applicability to different mineral systems, investigate long-term economic and environmental impacts, and focus on the flotation kinetics of coarse particles with microbubbles. Understanding the kinetic aspects could provide crucial insights into the bubble-particle interactions and the flotation efficiency. Further investigation of mechanisms underlying microbubble, cationic collector, and coarse particle interactions could advance the flotation technology. This work redefines the approaches to coarse particle

flotation, emphasizing the holistic optimization strategies, and opening new avenues for kinetic studies, paving the way for more efficient and sustainable mineral processing techniques.

References

[1]. B.A. Wills, J. Finch (2015). Wills' mineral processing technology: an introduction to the practical aspects of ore treatment and mineral recovery, Butterworth-heinemann.

[2]. S. Farrokhpay, L. Filippov, D. Fornasiero (2021). Flotation of fine particles: A review, *Mineral Processing and Extractive Metallurgy Review,* 42, 473–483.

[3]. D. Tao (2005). Role of Bubble Size in Flotation of Coarse and Fine Particles - A Review, *Sep Sci Technol,* 39, 741–760.

[4]. C. Gontijo, D. Fornasiero, J. Ralston (2008). The Limits of Fine and Coarse Particle Flotation, *Can J Chem Eng,* 85, 739–747.

[5]. G.J. Jameson (2010). Advances in Fine and Coarse Particle Flotation, *Canadian Metallurgical Quarterly,* 49, 325–330.

[6]. S. Ata, G.J. Jameson (2013). Recovery of coarse particles in the froth phase–A case study, *Miner Eng,* 45, 121–127.

[7]. D. Xu, I. Ametov, S.R. Grano (2011). Detachment of coarse particles from oscillating bubbles—The effect of particle contact angle, shape and medium viscosity, *Int J Miner Process,* 101, 50–57.

[8]. A. Hassanzadeh, M. Safari, D.H. Hoang, H. Khoshdast, B. Albijanic, P.B. Kowalczuk (2022). Technological assessments on recent developments in fine and coarse particle flotation systems, *Miner Eng,* 180.

[9]. S. Nazari, A. Hassanzadeh, Y. He, H. Khoshdast, P.B. Kowalczuk (2022). Recent Developments in Generation Detection and Application of Nanobubbles in Flotation, *Minerals 12*.

[10]. S. Farrokhpay, I. Ametov, S. Grano (2011). Improving the recovery of low grade coarse composite particles in porphyry copper ores, in: *Advanced Powder Technology*, pp. 464–470.

[11]. V. Kromah, S.B. Powoe, R. Khosravi, A.A. Neisiani, S.C. Chelgani (2022). Coarse particle separation by fluidized-bed flotation: A comprehensive review, *Powder Technol* 409.

[12]. S.J. Anzoom, G. Bournival, S. Ata (2024). Coarse particle flotation: A review, *Miner Eng*, 206, 108499.

[13]. S. Nazari, A. Hassanzadeh (2020). The effect of reagent type on generating bulk sub-micron (nano) bubbles and flotation kinetics of coarse-sized quartz particles, *Powder Technol*, 374, 160–171.

[14]. S. Nazari, S. Chehreh Chelgani, S.Z. Shafaei, B. Shahbazi, S.S. Matin, M. Gharabaghi (2019). Flotation of coarse particles by hydrodynamic cavitation generated in the presence of conventional reagents, *Sep Purif Technol* 220, 61–68.

[15]. M. Fan, Y. Zhao, D. Tao (2012). Fundamental studies of nanobubble generation and applications in flotation, *Separation Technologies for Minerals, Coal, and Earth Resources*, 457–469.

[16]. S. Nazari, S.Z. Shafaei, B. Shahbazi, S. Chehreh Chelgani (2018). Study relationships between flotation variables and recovery of coarse particles in the absence and presence of nanobubble, *Colloids Surf A Physicochem Eng Asp*, 559, 284–288.

[17]. D. Tao (2022). Recent advances in fundamentals and applications of nanobubble enhanced froth flotation: A review, *Miner Eng*, 183, 107554.

[18]. S. Zhou, Y. Li, S. Nazari, X. Bu, A. Hassanzadeh, C. Ni, Y. He, G. Xie (2022). An assessment of the role of combined bulk micro- and nano-bubbles in quartz flotation, *Minerals, 12*, 944.

[19]. L.O. Filippov, I.V. Filippova, V. V Severov (2010). The use of collector mixture in the reverse cationic flotation of magnetite ore: The role of Fe-bearing silicates, *Miner Eng*, 23, 91–98.

[20]. M.C. Fuerstenau, G.J. Jameson, R.-H. Yoon (2007). Froth flotation: a century of innovation, SME.

[21]. A. Vidyadhar, K.H. Rao, I. V Chernyshova, Pradip, K.S.E. Forssberg (2002). Mechanisms of Amine–Quartz Interaction in the Absence and Presence of Alcohols Studied by Spectroscopic Methods, *J Colloid Interface Sci*, 256, 59–72.

[22]. A.M. Nowosielska, A.N. Nikoloski, D.F. Parsons (2022). Interactions between coarse and fine galena and quartz particles and their implications for flotation in NaCl solutions, *Miner Eng*, 183, 107591.

[23]. C. Zhou, L. Liu, J. Chen, F. Min, F. Lu (2022). Study on the influence of particle size on the flotation separation of kaolinite and quartz, *Powder Technol*, 408, 117747.

[24]. E.H. Girgin, S. Do, C.O. Gomez, J.A. Finch (2006). Bubble size as a function of impeller speed in a self-aeration laboratory flotation cell, *Miner Eng*, 19, 201–203.

[25]. W.X. Weimin Xie, D.H. Dongsheng He, S.L. Shuang Liu, F.C. Fei Chen, H.L. Hongqiang Li (2020). Effect of pH and Dodecylamine Concentration on the Properties of Dodecylamine Two-Phase foam, *Journal of the Chemical Society of Pakistan*, 42, 495–495.

[26]. G. Fan, L. Wang, Y. Cao, C. Li (2020). Collecting agent–mineral interactions in the reverse flotation of iron ore: A brief review, *Minerals*, 10, 681.

[27]. B.K. Gorain, J.P. Franzidis, E. V Manlapig (1997). Studies on impeller type, impeller speed and air flow

rate in an industrial scale flotation cell. Part 4: Effect of bubble surface area flux on flotation performance, *Miner Eng*, 10, 367–379.

[28]. G.J. Jameson, A. V Nguyen, S. Ata (2007). The flotation of fine and coarse particles, Froth Flotation: A Century of Innovation, 339–372.

[29]. K.-A. Duffy, K. Runge, E. Tabosa (2013). Strategies for increasing coarse particle flotation in conventional flotation cells.

[30]. R.M. Rahman, S. Ata, G.J. Jameson (2012). The effect of flotation variables on the recovery of different particle size fractions in the froth and the pulp, *Int J Miner Process*, 106–109, 70–77.

[31]. R. Ahmadi, D.A. Khodadadi, M. Abdollahy, M. Fan (2014). Nano-microbubble flotation of fine and ultrafine chalcopyrite particles, *Int J Min Sci Technol*, 24, 559–566.

[32]. B. Elvers (1991). Ullmann's encyclopedia of industrial chemistry, Verlag Chemie Hoboken, NJ.

[33]. Y.S. Cho, J.S. Laskowski (2002). Effect of flotation frothers on bubble size and foam stability, *Int J Miner Process*, 64, 69–80.

[34]. J.G. Wiese, P.J. Harris, D.J. Bradshaw (2010). The effect of increased frother dosage on froth stability at high depressant dosages, in: *Miner Eng*, pp. 1010–1017.

[35]. S. Nazari, S. Chehreh Chelgani, S.Z. Shafaei, B. Shahbazi, S.S. Matin, M. Gharabaghi (2019). Flotation of coarse particles by hydrodynamic cavitation generated in the presence of conventional reagents, *Sep Purif Technol*, 220, 61–68.

[36]. Y. Li, F. Wu, W. Xia, Y. Mao, Y. Peng, G. Xie (2020). The bridging action of microbubbles in particle-bubble adhesion, *Powder Technol*, 375, 271–274.

[37]. S. Nazari, S.Z. Shafaei, M. Gharabaghi, R. Ahmadi, B. Shahbazi (2018). Effect of frother type and operational parameters on nano bubble flotation of quartz coarse particles, *Journal of Mining & Environment*, 9, 539–546.

[38]. H. Darabi, S.M.J. Koleini, D. Deglon, B. Rezai, M. Abdollahy (2019). Investigation of bubble-particle interactions in a mechanical flotation cell, part 1: Collision frequencies and efficiencies, *Miner Eng*, 134, 54–64.

[39]. S. Farrokhpay, D. Fornasiero (2017). Flotation of coarse composite particles: Effect of mineral liberation and phase distribution, *Advanced Powder Technology*, 28, 1849–1854.

[40]. D. Wang, Q. Liu (2021). Hydrodynamics of froth flotation and its effects on fine and ultrafine mineral particle flotation: A literature review, *Miner Eng*, 173.

[41]. A.M. Vieira, A.E.C. Peres (2007). The effect of amine type, pH, and size range in the flotation of quartz, *Miner Eng*, 20, 1008–1013.

[42]. C. Bazin, M.P. Proulx (2001). Distribution of reagents down a flotation bank to improve the recovery of coarse particles. www.elsevier.nlrlocaterijminpro.

[43]. J. Rubio, A. Azevedo, R.T. Rodrigues, G.R. Olivares (2024). Amine-coated nanobubbles-assisted flotation of fine and coarse quartz, *Miner Eng*, 218, 108983.

[44]. S. Nazari, A. Hassanzadeh (2020). The effect of reagent type on generating bulk sub-micron (nano) bubbles and flotation kinetics of coarse-sized quartz particles, *Powder Technol*, 374, 160–171.

[45]. S. Nazari, S.Z. Shafaei, M. Gharabaghi, R. Ahmadi, B. Shahbazi, A. Tehranchi (2020). New approach to quartz coarse particles flotation using nanobubbles, with emphasis on the bubble size distribution, *Int J Nanosci*, 19, 1850048.

فرضیات چالش برانگیز ریزحباب: مدل سازی و بهینه سازی فلوتاسیون کوارتز درشت در یک محیط کاتیونی

احمد آبباکر[۱،۳*]، و نوذت اصلان[۲]

۱- گروه مهندسی معدن، دانشکده تحصیلات تکمیلی علوم طبیعی و کاربردی، دانشگاه سیواس جمهوریت، ۵۸۱۴۰ سیواس، ترکیه

۲- گروه مهندسی صنایع، دانشگاه سیواس جمهوریت، ۵۸۱۴۰ سیواس، ترکیه

۳- گروه مهندسی معدن، دانشکده علوم فنی، دانشگاه اسلامی عمران، خارطوم، اومدورمان، سودان

ارسال ۲۰۲۴/۰۸/۰۹، پذیرش ۲۰۲۴/۱۱/۱۸

* نویسنده مسئول مکاتبات: a7medelmubarak@oiu.edu.sd

چکیده:

این کار فلوتاسیون ذرات درشت را با استفاده از شناورسازی به کمک میکروحباب در یک محیط کاتیونی ایجاد شده توسط دودسیلامین (DDA) بهینه می کند. راندمان شناورسازی ذرات کوارتز درشت (D50 = 495 میکرومتر) از طریق بررسی برهمکنش‌های بین میکروحباب‌ها (۲۰-۳۰ میکرومتر)، محیط کاتیونی، و پارامترهای عملیاتی مختلف مورد بررسی قرار گرفت. یک رویکرد سیستماتیک با استفاده از طرح‌های آزمایشی فاکتوریل و باکس-بنکن برای ارزیابی اثرات متغیرهای چندگانه مورد استفاده قرار گرفت. این متغیرها شامل غلظت دودسیلامین (DDA)، غلظت متیل ایزوبوتیل کاربینول (MIBC)، سرعت پروانه، چگالی خمیر، افزودن ذرات ریز و وجود میکروحباب‌ها بود. غلظت DDA و سرعت پروانه به طور قابل‌توجهی بر بازیابی ذرات درشت تأثیر گذاشت، در حالی که میکروحباب‌ها در شرایط غیر بهینه، بازیابی را ۱۵ درصد افزایش دادند. بهینه سازی تفاوت ناچیزتری را نشان داد. شرایط بهینه شده به ترتیب به حداکثر بازیابی ۹۹.۴۷٪ و ۹۷.۸۸٪ با و بدون میکروحباب دست یافت که نشان دهنده حداقل اثر زمانی که سایر پارامترها بهینه شدند. این کار تحقیقاتی نشان می‌دهد که یک بهینه‌سازی دقیق پارامترهای شناورسازی می‌تواند به نرخ‌های بازیابی ذرات درشت بالایی دست یابد، با میکروحباب‌ها نقش کمتری نسبت به پیش‌بینی‌شده بازی می‌کنند. این یافته‌ها نشان می‌دهد که بهینه‌سازی پارامترهای معمولی ممکن است بسیار مهم‌تر از معرفی میکروحباب برای افزایش کارایی شناورسازی ذرات بزرگ‌تر باشد. این کار به درک ما از شناورسازی ذرات درشت کمک می‌کند و بینش‌هایی را برای بهبود تکنیک‌های پردازش مواد معدنی برای به چالش کشیدن اندازه ذرات ارائه می‌کند.

کلمات کلیدی: شناورسازی ذرات درشت، شناورسازی به کمک ریزحباب، محیط کاتیونی، بهینه‌سازی، مدل‌سازی.